

Tracing magnetic fields in star-forming regions on multiple scales



S. Reissl¹, S. Wolf¹, D. Seifried², R. Banerjee³

¹Universität zu Kiel, Institut für Theoretische Physik und Astrophysik, Leibnizstraße 15, 24118 Kiel, Germany

²Universität zu Köln, I. Physikalisches Institut, Zùlpicher Straße 77, 50937 Köln, Germany

³Hamburger Sternwarte, Gojenbergsweg 112, 21029 Hamburg, Germany

e-mail: sreissl@astrophysik.uni-kiel.de, wolf@astrophysik.uni-kiel.de



Introduction

We investigate the potential of continuum polarization measurements to constrain the impact of magnetic fields on star-formation in the interstellar medium (ISM) from collapsing molecular clouds to circumstellar disks by post-processing complex magnetic field, temperature, and density distributions as well as velocity fields resulting from magnetohydrodynamic (MHD) simulations. Our approach is to create synthetic polarization maps by combining radiative transfer and polarization algorithms with state of the art dust grain alignment theories.

1. Radiative Transfer Code

We developed an extended version of the 3D Monte-Carlo (MC) radiative transfer code MC3D (Wolf et al., 1999, 2000; Reissl et al., 2014b submitted).

- **Radiation sources:** Arbitrary number of point (stars), diffuse, and background sources, and thermal dust reemission
- **MC dust heating:** Combined heating algorithm of continuous absorption (Lucy 1999) and immediate temperature correction (Bjorkman & Wood 2001)
- **Grid:** Octree-grid with adaptive level refinement
- **Polarization mechanism:** Dichroic extinction, thermal reemission, and scattering (Whitney & Wolff 2002)
- **Dust grain alignment:** Various alignment mechanisms (see below)
- **Optimization:** Enforced scattering, wavelength range selection (Wolf et al., 2000), and modified random walk (Min et al., 2009)

2. Dust model and grain alignment

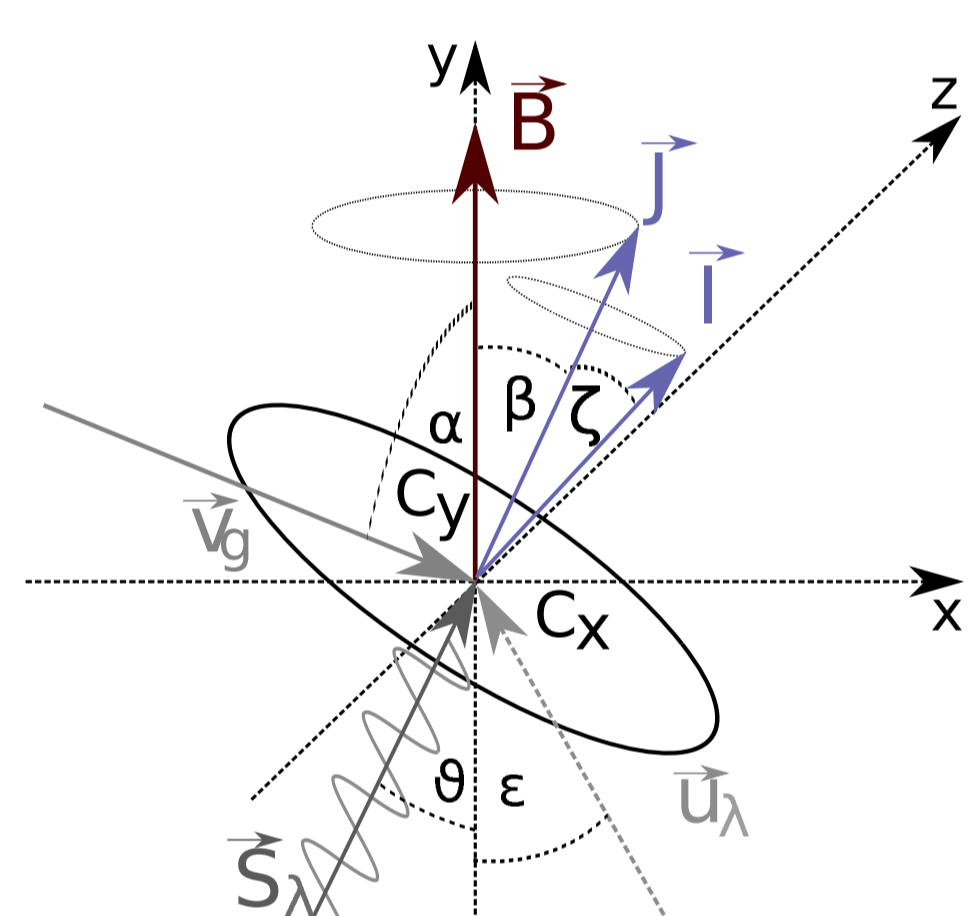


Fig. 1: Dust grains precess with angular momentum \vec{J} around the magnetic field \vec{B} and with moment of inertia \vec{I} around \vec{J} (internal alignment) leading to a lower degree of polarization. This depends on the anisotropy of the radiation field \vec{u}_λ , gas streams \vec{v} , and the incident light \vec{S} .

The optical properties of the dust grains are calculated by applying the Discrete Dipole Approximation (DDA) implemented in the program DDSCAT 7.2 (Draine & Flatau 2012).

- **Material:** Astrosilicate and graphite
- **Shape:** Oblate, aspect ratio of 1/2
- **Wavelength:** 90 nm – 2 mm
- **Grain size:** $a \in [5 \text{ nm} - 2 \mu\text{m}]$
- **Size distribution:** $n(a) \propto a^{-3.5}$
- **Mass fraction:** $M_{\text{gas}}/M_{\text{dust}} = 100$
- **Polarization cross section:** $C_{\text{pol}} = R \times (C_x - C_y) \sin^2(\vartheta)$
- **Rayleigh reduction factor:** $R = \langle (1.5 \cos^2(\beta) - 0.5) (1.5 \cos^2(\zeta) - 0.5) \rangle$

We make predictions for the case of imperfect grain alignment, taking following mechanisms into account:

- **Imperfect Davis-Greenstein (IDG):** Paramagnetic relaxation (Davis & Greenstein 1951; Voshchinnikov 2010)
- **Radiative torques (RAT):** Radiation-dust interaction (Lazarian 2007)
- **Mechanical alignment (GOLD):** Alignment by gas streams (Gold 1952; Lazarian 1994)

3. The impact of dust alignment mechanisms on polarization

We compare several alignment mechanisms in a complex MHD environment to examine their contribution to polarization. Each mechanism results in characteristic patterns of linear polarization.

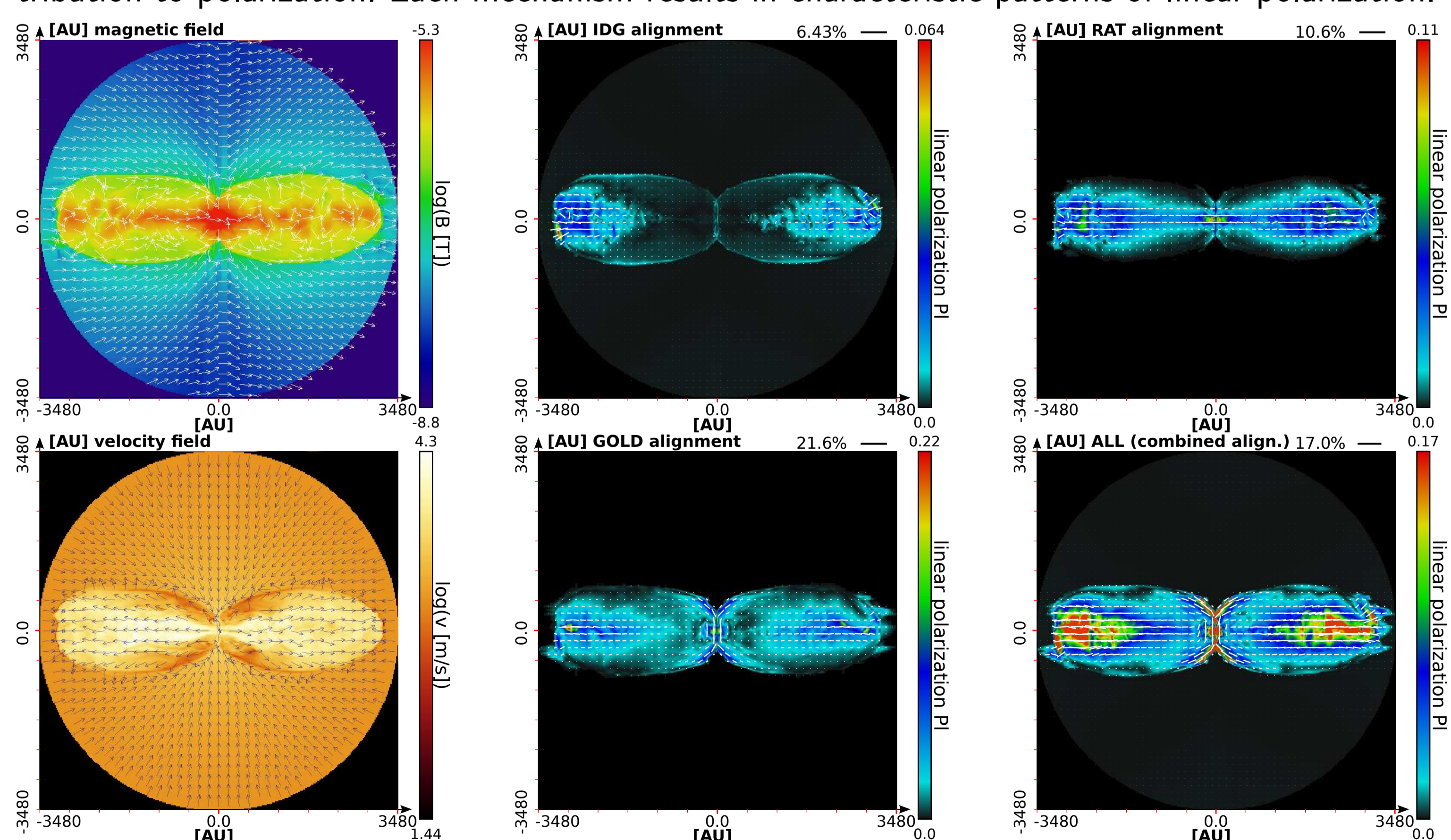


Fig. 2: Magnetic (top left) and velocity field (bottom left) of a MHD simulation with $100 M_\odot$ after 5 kyr. An accretion disk, six stars in the center, and outflows in the surrounding ISM have formed. The dust temperature was calculated with our MC code. Linear polarization maps were calculated for IDG (top center), GOLD (bottom center), RAT (top left), and the combination of all mechanisms (left bottom) at a wavelength of 1 mm. [from Reissl et al., 2014c]

4. The potential of submillimeter polarization measurements

We evaluate the potential of polarization measurements to constrain the magnetic field morphology in circumstellar disks by considering RAT alignment and heating by a central star. The density distribution (Shakura & Sunyaev 1973) follows:

$$\frac{\alpha}{2.6} \frac{\beta}{1.25} \frac{h_0[\text{AU}]}{10} \frac{r_0[\text{AU}]}{100} \frac{R_{\text{in}}[\text{AU}]}{30} \frac{R_{\text{out}}[\text{AU}]}{270} \frac{M_{\text{disk}}[M_\odot]}{10^{-5} \& 10^{-3}} \rho_{\text{dust}}(r, z) \propto \left(\frac{r_0}{r}\right)^\alpha \exp\left(-\frac{1}{2} \left[\frac{z}{h_0} \left(\frac{r_0}{r}\right)^\beta\right]^2\right)$$

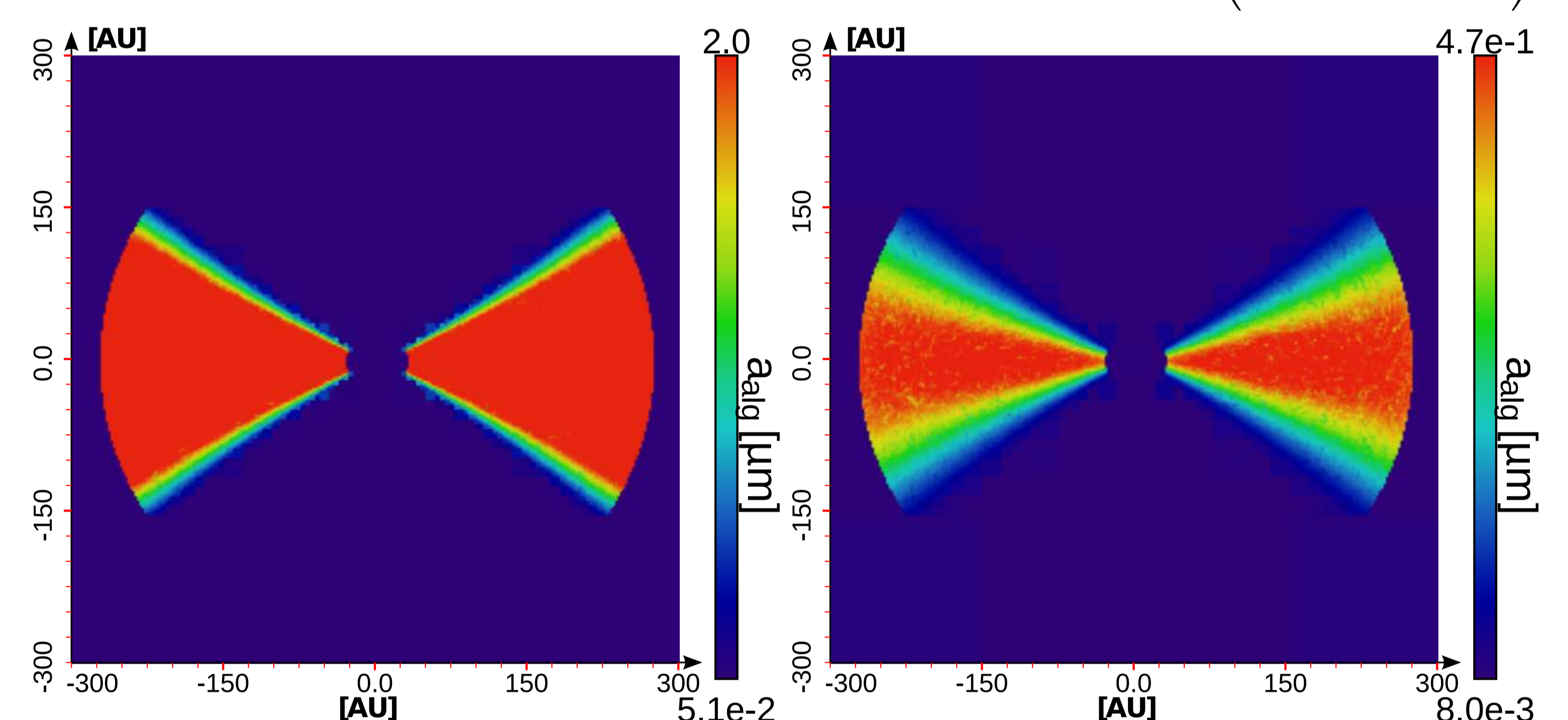


Fig. 3: Distribution of grain sizes a_{dust} where dust particles start to align with \vec{B} according to RAT theory because of an anisotropic radiation field in the plane perpendicular to the mid-plane. Total disk masses are $10^{-5} M_\odot$ (left) and $10^{-3} M_\odot$ (right). Lower a_{dust} result in higher degrees of polarization. [from Reissl et al., 2014b]

RAT alignment depends on dust temperature and density. With increasing disk mass RAT alignment should produce detectable amount of linear polarization in the mid-infrared and sub-mm, allowing to infer the underlying magnetic field morphology.

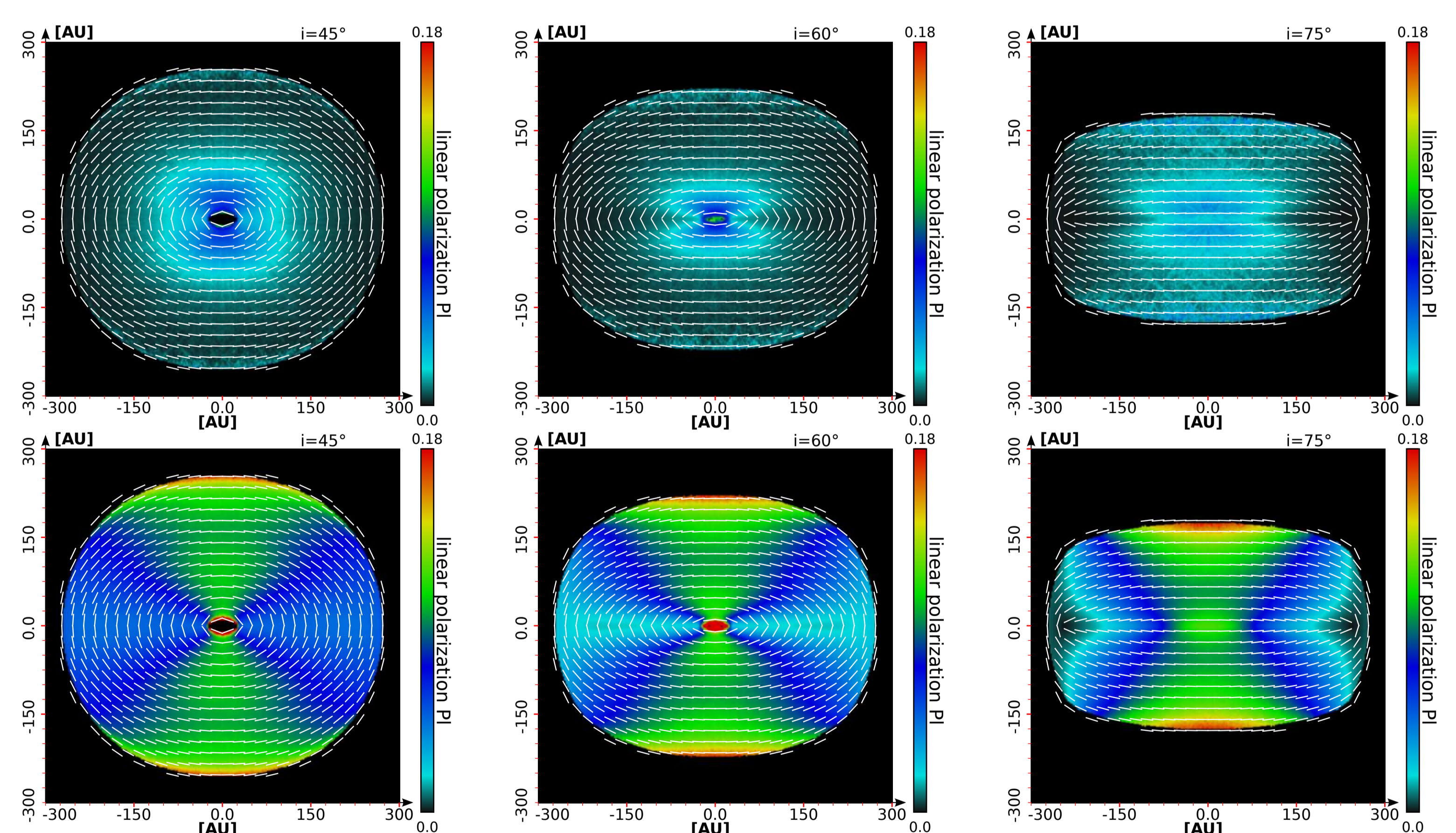


Fig. 4: Maps of linear polarization overlaid with normalized orientation vectors at a wavelength of $515 \mu\text{m}$ of disks with total masses are $10^{-5} M_\odot$ (top row) and $10^{-3} M_\odot$ (bottom row) a toroidal 3D magnetic field morphology at inclination angles of 45° (left), 60° (middle), and 75° (right). The dust grains are imperfectly aligned with the RAT mechanism. Polarization vectors have an offset of 90° to match the projected magnetic field. [from Reissl et al., 2014b]

5. Conclusion

- Dust alignment mechanisms influence the patterns of linear polarization in a unique way allowing to identify the dominant alignment mechanism in star forming regions on multiple scales.
- Circumstellar disk models considering RAT alignment are consistent with observations and can bridge the gap between observational data and theoretical predictions.

Literature:

Bjorkman, J. E. & Wood, K. 2001, *AJ*, 122, 615
 Voshchinnikov, N. V., Hoang, T., & V. B. 2010, *MNRAS*, 404, 265
 Davis, Jr., L. & Greenstein, J. L. 1951, *AJ*, 114, 206
 Draine, B. T. & Flatau, P. J. 2012, *arXiv preprint*
 Gold, T. 1952, *MNRAS*, 112, 215
 Lazarian, A. 1994, *MNRAS*, 268, 713
 Lucy, L. B. 1999, *A&A*, 344, 282
 Min, M. et al., J. W. 2009, *A&A*, 497, 155
 Reissl, S., Wolf, S., & Seifried, D. 2014a, *A&A*, 566, A65
 Reissl, S. & Wolf, S. 2014b submitted
 Reissl, S., Wolf, S., Seifried, D. 2014c in prep.
 Shakura, N. I. & Sunyaev, R. A. 1973, *A&A*, 11, 1491
 Whitney, B. A. & Wolff, M. J. 2002, *AJ*, 124, 205
 Wolf, S., Henning, T. 2000, *CPC*, 132, 166
 Wolf, S., Henning, T., & Stecklum, B. 1999, *A&A*, 349, 839